FEEDBACK OPERATION OF CHOPPER-CONTROLLED INDUCTION MOTOR

M.Y. ABDELFATTAH
Electrical Engineering Department,
Faculty of Engineering,
Alexandria University,
Alexandria, EGYPT

ABSTRACT

In this paper, the speed of an induction motor is controlled by controlling its slip energy using a chopper circuit on the rotor side. Analysis and simulation consider the induction motor equations from the rotor side where a diode bridge is connected. The open-loop control has a very poor speed response. Therefore, it is essential to employ a closed-loop speed control. A closed-loop control system is suggested, where a permanent magnet tachogenerator is mounted on the rotor shaft to provide a dc signal proportional to the rotor speed to the feedback control scheme. The advantage of the new method of analysis is that it allows the study of system dynamic response associated with large signal perturbations. The system response was studied by varying the feedback closed-loop gain. Also the effect of varying the load torque was taken into consideration.

NOTATIONS

A,B,C	Suffices indicating stator variables as in v_A
a,b,c	Suffices indicating rotor variables as in v_a
s	Suffix indicating stator quantity as in L_s
r	Suffix indicating rotor quantity as in L_r
q,d	Suffices indicating q and d axes respectively
i_{qs},i_{ds}	q,d axes equivalent stator currents
i_{qr},i_{dr}	q,d axes equivalent rotor currents
v_{qs},v_{ds}	q,d axes equivalent stator voltages
v_{qr},v_{dr}	q,d axes equivalent rotor voltages
R_s	Resistance of stator phase winding
R_r	Resistance of rotor phase winding
L_s	Stator self inductance per phase
L_r	Rotor self inductance per phase
M	Mutual inductance between stator and rotor windings per phase
ω_r	Rotor angular speed
θ	Angle between stator phase A and rotor phase a
J	Rotor moment of inertia
T_E	Electromagnetic torque developed
T_L	Load torque
T_D	Damping torque
R_{add}	Added resistance to rotor side
R_F,L_F	Filter resistance and inductance respectively
T_{CH}	The chopper chopping period
T_{ON}	The chopper on period
λ	The chopper duty cycle ($\lambda = T_{ON} / T_{CH}$)
i_{link}	Instantaneous link (filter) current
p	Operator d/dt

Note : all quantities are in per unit

INTRODUCTION

Connection of resistors to the slip-rings of an induction motor can improve starting conditions and give speed adjustment. Different attempts have been made to use SCR's in different configurations in the rotor circuit to have continuous and contactless effective rotor impedance control [1-4]. In references [2-4] the effective rotor resistance is controlled by varying the duty cycle of the chopper. This technique is easy to use for closed loop control systems. Figure (1), shows the system suggested for study. In this system, the filter is used to minimize the harmonic contents in the ac component of the rectified rotor current.

In reference [2] the dynamic response based on a dc circuit model was obtained for this particular drive which can be used for studying closed-loop drive performance. However, this dynamic model was only for a small signal

perturbations.

In a previous paper by the author [5], the analysis of this system has been studied. However, the system performance was only studied with open-loop controller. The open-loop control showed a very poor speed response. Therefore, it is essential to employ a closed-loop control to improve the system response. The analysis used in [5] considers the induction motor equations from the rotor side where a diode bridge is connected and where these equations are solved taking the nonlinear devices (diodes) into account. This analysis gives us precise calculations for all system states without any approximations. Therefore, the system dynamics with the present of a closed-loop controller can be studied for small or large signal perturbations.

A proposed closed-loop controller is suggested, and the system response was studied for this controller. The system performance following a large signal disturbance was studied by varying the feedback closed-loop gain. Also, the effect of varying the load torque was taken into consideration.

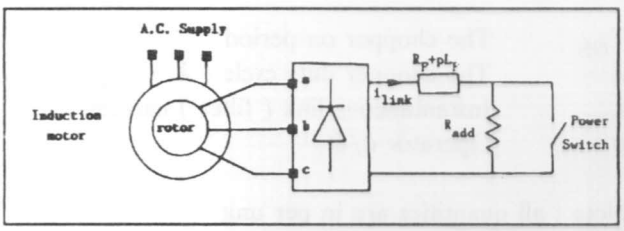

Figure 1. Chopper-controlled induction motor.

INDUCTION MACHINE EQUIVALENT CIRCUIT REFERRED TO ROTOR USING D-Q MODEL

The study of the transient performance of three phase induction motors and their behaviour on non-sinusoidal supplies is much easier with transformation of the machine variables to a reference frame in which there is a stationary reference frame. They are called the direct and quadrature, axes [6]. Since the choice of time-zero is arbitrary, it is most convenient to choose time-zero at the instant when q,A and a axes are all coincident as shown in Figure (2). Choosing an instant when the α-axis of the rotating two phase axes (α,β) makes an angle θ with the stationary q-axis, and assuming no zero-sequence components, one form of transformation of rotor quantities between rotating three-phase (a,b,c) and stationary two-phase (q,d) is :

$$\begin{bmatrix} v_a \\ v_b \\ v_c \end{bmatrix} = \begin{bmatrix} \cos\theta & -\sin\theta \\ \cos(\theta+120^o) & -\sin(\theta+120^o) \\ \cos(\theta-120^o) & -\sin(\theta-120^o) \end{bmatrix} \begin{bmatrix} v_{qr} \\ . \\ v_{dr} \end{bmatrix} \quad (1)$$

and

$$\begin{bmatrix} i_a \\ i_b \\ i_c \end{bmatrix} = \begin{bmatrix} \cos\theta & -\sin\theta \\ \cos(\theta+120^o) & -\sin(\theta+120^o) \\ \cos(\theta-120^o) & -\sin(\theta-120^o) \end{bmatrix} \begin{bmatrix} i_{qr} \\ . \\ i_{dr} \end{bmatrix} \quad (2)$$

Also, we can define the (d,q) stator voltages as:

$$\begin{bmatrix} v_{qs} \\ \\ v_{ds} \end{bmatrix} = \begin{bmatrix} 1 & 0 & 0 \\ 0 & -\frac{1}{\sqrt{3}} & \frac{1}{\sqrt{3}} \end{bmatrix} \begin{bmatrix} v_A \\ v_B \\ v_C \end{bmatrix} \quad (3)$$

The above transformations do not give invariance of power, but this is not important in this case since variables are ultimately expressed in the three-phase reference frame.

Using per-unit quantities, the differential equations describing the behaviour of the machine when referred to the stationary frame can be written in the form :

$$\begin{bmatrix} v_{qs} \\ v_{ds} \\ v_{qr} \\ v_{dr} \end{bmatrix} = \begin{bmatrix} R_s & 0 & 0 & 0 \\ 0 & R_s & 0 & 0 \\ 0 & -\omega_r M & R_r & -\omega_r L_r \\ \omega_r M & 0 & \omega_r L_r & R_r \end{bmatrix} \begin{bmatrix} i_{qs} \\ i_{ds} \\ i_{qr} \\ i_{dr} \end{bmatrix} + \begin{bmatrix} L_s & 0 & M & 0 \\ 0 & L_s & 0 & M \\ M & 0 & L_r & 0 \\ 0 & M & 0 & L_r \end{bmatrix} p \begin{bmatrix} i_{qs} \\ i_{ds} \\ i_{qr} \\ i_{dr} \end{bmatrix} \quad (4)$$

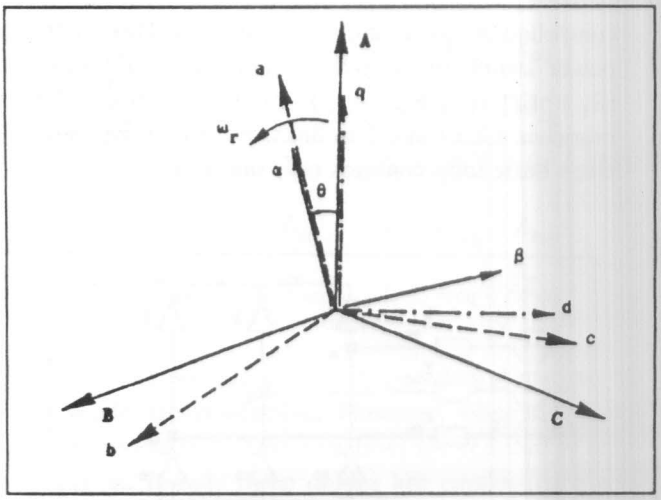

Figure 2. Different machine phase axes.

which is in the form :

$$V = [R]\, i + [L]\, pi$$

and can be rewritten in the form :

$$pi = [L]^{-1} \{ V - [R]\, i \}$$

from which we can get the following derivatives :

$$\begin{aligned}
pi_{qs} &= [L_r v_{qs} - M v_{qr} - \omega_r M^2 i_{ds} - \omega_r M L_r i_{dr} \\
&\quad - L_r R_s i_{qs} + M R_r i_{qr}] / (L_r L_s - M^2) \\
pi_{ds} &= [L_r v_{ds} - M v_{dr} + \omega_r M^2 i_{qs} + \omega_r M L_r i_{qr} \\
&\quad - L_r R_s i_{ds} + M R_r i_{dr}] / (L_r L_s - M^2) \\
pi_{qr} &= [-M v_{qs} + L_s v_{qr} + \omega_r L_s M i_{ds} + \omega_r L_s L_r i_{dr} \\
&\quad + M R_s i_{qs} - L_s R_r i_{qr}] / (L_r L_s - M^2) \\
pi_{dr} &= [-M v_{ds} + L_s v_{dr} - \omega_r M L_s i_{qs} - \omega_r L_s L_r i_{qr} \\
&\quad + M R_s i_{ds} - L_s R_r i_{dr}] / (L_r L_s - M^2)
\end{aligned} \tag{5}$$

In per-unit quantities the electromagnetic torque T_E becomes :

$$T_E = M [i_{dr}\, i_{qs} - i_{qr}\, i_{ds}] \tag{6}$$

The conventional form of writing the balance between input and output in per-unit is in the form :

$$T_E = 2H\, p\omega_r + T_D + T_L$$

where H is the motor inertia constant in seconds. However, according to the selected base quantities given in Appendix (A), this equation will be in the form :

$$T_E = J\, p\omega_r + T_D + T_L \tag{7}$$

Equation (7) can be rearranged as :

$$p\omega_r = [T_E - T_L - T_D] / J \tag{8}$$

$$p\theta = \omega_r \tag{9}$$

Substituting equations (4) and (5) into equation (1) and then substituting for i_{qr} & i_{dr} using equation (2) we get :

$$\begin{aligned}
v_a &= [R_r + pL_{eq}] i_a + [\omega_r (L_{eq} - L_r) i_{dr} - \omega_r M i_{ds} - (MR_s/L_s) i_{qs} \\
&\quad + (M/L_s) v_{qs}] \cos\theta - [\omega_r (L_r - L_{eq}) i_{qr} + \omega_r M i_{qs} \\
&\quad - (MR_s/L_s) i_{ds} + (M/L_s) v_{ds}] \sin\theta
\end{aligned} \tag{10}$$

$$\begin{aligned}
v_b &= [R_r + pL_{eq}] i_b + [\omega_r (L_{eq} - L_r) i_{dr} - \omega_r M i_{ds} - (MR_s/L_s) i_{qs} \\
&\quad + (M/L_s) v_{qs}] \cos(\theta + 120^\circ) - [\omega_r (L_r - L_{eq}) i_{qr} + \omega_r M i_{qs} \\
&\quad - (MR_s/L_s) i_{ds} + (M/L_s) v_{ds}] \sin(\theta + 120^\circ)
\end{aligned} \tag{11}$$

$$\begin{aligned}
V_c &= [R_r + pL_{eq}] i_c + [\omega_r (L_{eq} - L_r) i_{dr} - \omega_r M i_{ds} - (MR_s/L_s) i_{qs} \\
&\quad + (M/L_s) v_{qs}] \cos(\theta - 120^\circ) - [\omega_r (L_r - L_{eq}) i_{qr} + \omega_r M i_{qs} \\
&\quad - (MR_s/L_s) i_{ds} + (M/L_s) v_{ds}] \sin(\theta - 120^\circ)
\end{aligned} \tag{12}$$

where;

$$L_{eq} = (L_r L_s - M^2)/L_s \tag{13}$$

Equations (10)-(12) can be represented by the equivalent circuit shown in Figure (3), where;

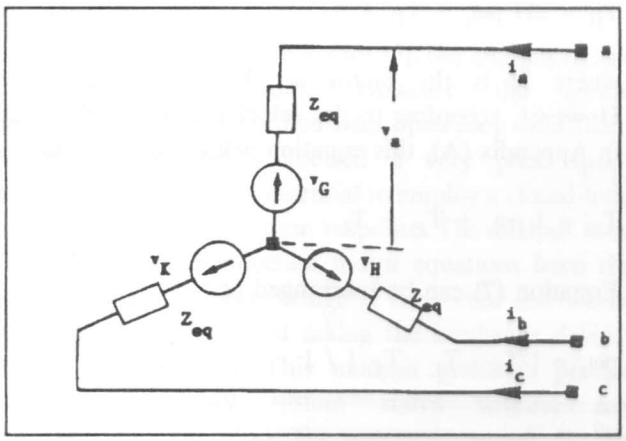

Figure 3. Equivalent circuit for an induction machine referred to rotor side.

$$v_G = [\omega_r(L_{eq}-L_r)i_{dr}-\omega_r M i_{ds}-(MR_s/L_s)i_{qs} + (M/L_s)v_{qs}]\cos\theta - [\omega_r(L_r-L_{eq})i_{qr}+\omega_r M i_{qs} -(MR_s/L_s)i_{ds}+(M/L_s)v_{ds}]\sin\theta \quad (14)$$

$$v_H = [\omega_r(L_{eq}-L_r)i_{dr}-\omega_r M i_{ds}-(MR_s/L_s)i_{qs} + (M/L_s)v_{qs}]\cos(\theta+120^\circ) - [\omega_r(L_r-L_{eq})i_{qr}+\omega_r M i_{qs} -(MR_s/L_s)i_{ds}+(M/L_s)v_{ds}]\sin(\theta+120^\circ) \quad (15)$$

$$v_K = [\omega_r(L_{eq}-L_r)i_{dr}-\omega_r M i_{ds}-(MR_s/L_s)i_{qs} + (M/L_s)v_{qs}]\cos(\theta-120^\circ) - [\omega_r(L_r-L_{eq})i_{qr}+\omega_r M i_{qs} -(MR_s/L_s)i_{ds}+(M/L_s)v_{ds}]\sin(\theta-120^\circ) \quad (16)$$

$$Z_{eq} = [\, R_r + pL_{eq}] \quad (17)$$

ANALYSIS

Figure (4) shows a modified circuit for the chopper-controlled induction motor. During ON/OFF operation of power switch the equivalent impedance Z_L varies from $[R_F+pL_F]$ to $[(R_F+R_{add})+pL_F]$ respectively. Choosing branches 1,2,3,4 and 5 as links, we obtain five basic loops. Each basic loop contains only one link.

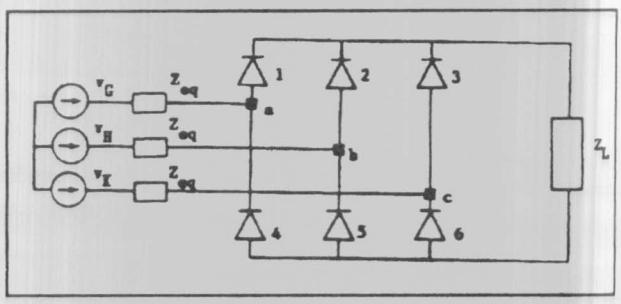

Figure 4. Modified circuit for chopper controlled induction motor.

The performance equation of the network in the loop reference frame [7] can be written in the form:

$$E_{loop} = Z_{loop}\, I_{loop} \quad (18)$$

from the previous choice of links we conclude that :

$$E_{loop} = \begin{bmatrix} v_G-v_K \\ v_H-v_K \\ 0 \\ v_G-v_K \\ v_H-v_K \end{bmatrix} \quad (19)$$

$$I_{loop} = \begin{bmatrix} I_1 \\ I_2 \\ I_3 \\ I_4 \\ I_5 \end{bmatrix} \quad (20)$$

$$Z_{loop} = \begin{bmatrix} Z_L+2Z_{eq} & Z_L+Z_{eq} & Z_L & 2Z_{eq} & Z_{eq} \\ Z_L+Z_{eq} & Z_L+2Z_{eq} & Z_L & Z_{eq} & 2Z_{eq} \\ Z_L & Z_L & Z_L & 0 & 0 \\ 2Z_{eq} & Z_{eq} & 0 & 2Z_{eq} & Z_{eq} \\ Z_{eq} & 2Z_{eq} & 0 & Z_{eq} & 2Z_{eq} \end{bmatrix} \quad (21)$$

Equation (18) represents five independent equations if the six diode are conducting. However, when only two diodes are conducting, these equations are reduced to only one equation. If only three diodes are conducting these equations are reduced to only two equations, etc. [8-9]. The situation of rectifier bridge can be defined in an array named rectifier state-array S having six elements, the individual elements being 1 or 0 depending on whether the diode is conducting or not respectively [7]. The matrix connecting the existing loops with those if all diodes are conducting is C_n. The construction of C_n is obtained from the previous knowledge of S [7]. The transformation process gives the voltage and currents vectors for the new networks as:

$$V_n = C_n^t E_{loop} \quad (22)$$

$$I_{loop} = C_n I_n \quad (23)$$

The new impedance matrix is given by:

$$Z_n = C_n^t Z_{loop} C_n \quad (24)$$

from which the following equation can be written:

$$V_n = Z_n I_n \quad (25)$$

Therefore,

$$V_n = [R_n + pL_n] I_n$$

and

$$pI_n = L_n^{-1} [V_n - R_n I_n] \quad (26)$$

which may be calculated at any time t giving the current derivatives at this instant.

When all six diodes are conducting the voltage drop across each of them is zero, and equation (18) holds good. However, if any diode is open, then a voltage will appear across it. It is necessary to calculate this voltage to check whether a new diode is to be included in the conducting pattern or not. To calculate this voltage, equation (18) will be modified to the form:

$$V_x = E_{loop} - Z_{loop} I_{loop} \quad (27)$$

From the previous choice of links, we find that diode number 6 is the dependent diode; then V_x is expressed as:

$$V_x = \begin{bmatrix} V_1+V_6 \\ V_2+V_6 \\ V_3+V_6 \\ -V_4+V_6 \\ -V_5+V_6 \end{bmatrix} \quad (28)$$

where V_j is the voltage across the jth diode.

Figure (5) shows a simplified flow chart for the proposed system analysis.

CONTROL SYSTEM

The block diagram of the feedback control scheme is given in Figure (6). The rotor speed of the motor gets adjusted with the variation of the duty cycle λ of the power switch. The tachogenerator output voltage is proportional to rotor speed ω_r and is compared with a dc voltage of fixed level which represents the set speed ω_{ref}. The error voltage is fed to the controller.

The simplest form of control is one in which the error signal e(t) is multiplied by a constant K_p to give a signal called the manipulated variable m(t) which is the input to the process. This arrangement is called proportional control, and by varying the value of K_p, the dynamic behaviour of the overall system can be altered [10]. For very low values of K_p, the response is likely to be sluggish. As K_p increases the response of the system for the same magnitude of error becomes more rapid and, if K_p is very large, instability is likely to result, or the oscillatory response would be so lightly damped.

Figure (7) shows the functional block diagram of the chopper-controlled drive using proportional control.

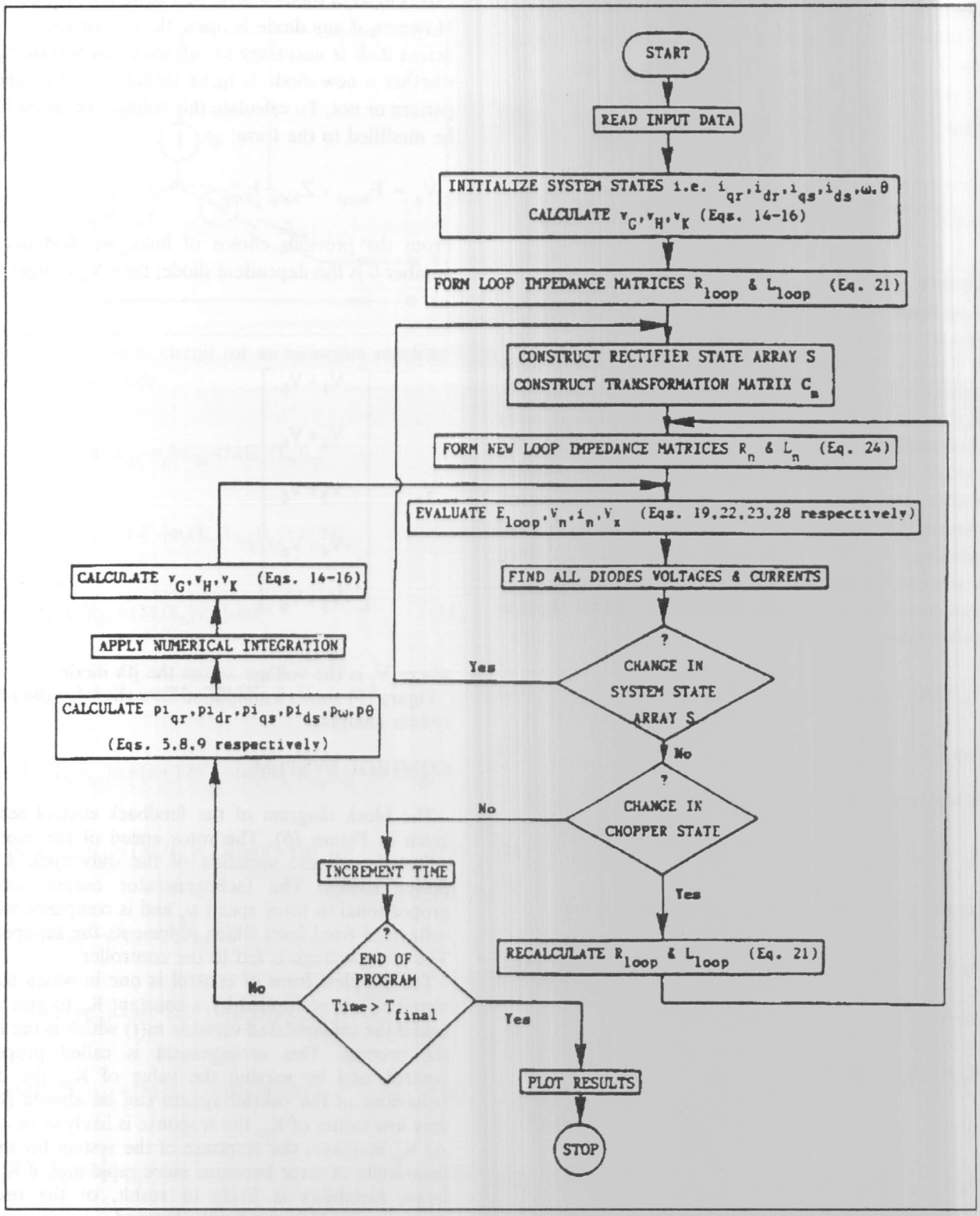

Figure 5. Simplified flow chart

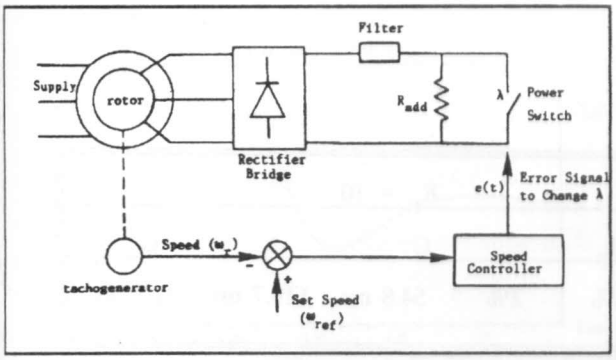

Figure 6. Block diagram of closed-loop system.

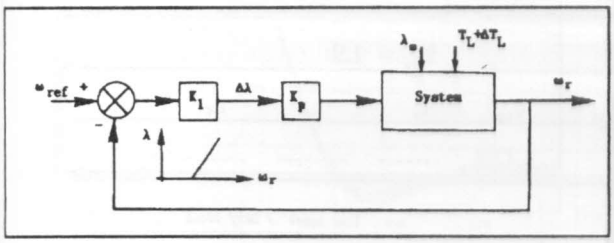

Figure 7. Functional block diagram.

NUMERICAL RESULTS

For the simulation results, Euler method of numerical integration was used. The time increment for numerical integration Δt was chosen to be 0.01 p.u. for the computer program execution. The system parameters in per-unit are given in Appendix (A). Figure (8) shows the relations between the speed of motor ω_r and chopper duty cycle λ for constant load torque T_L at steady-state. Figure (8) is extracted from reference [5].

The constant K_1 depends upon the operating point and is determined from the steady-state characteristic of the system. From Figure (8) it is clear that at steady-state the relationships between duty cycle and machine speed is nearly linear. Therefore, for a load torque T_L = 6 N.m the constant K_1 is found from:

$$K_1 = (0.75 - 0.6) / (1023 - 941) = 1.8292 \times 10^{-3} \text{ r.p.m.}^{-1}$$

and in per-unit :

$$K_1 = 1500 \times (1.8292 \times 10^{-3}) = 2.7439$$

The system was studied for two different strategies:

Constant Speed Drive:

by changing the load torque from 6 N.m to 8 N.m while the speed demand is 941 r.p.m. with λ_o = 0.6

Variable Speed Drive:

by fixing the load torque at 8 N.m while the speed command was changed from 718 r.p.m. to 833 r.p.m. with λ_o = 0.6.

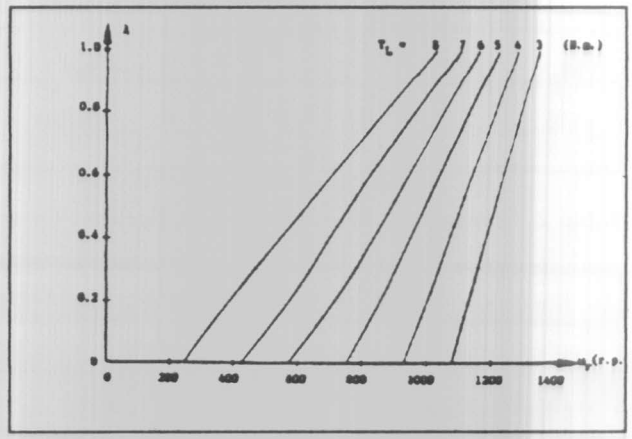

Figure 8. [Duty cycle/Speed] for different load torques at steady-state.

For all cases the machine was allowed to run for some time, here about 2 seconds, to reach steady-state before applying the disturbance at a time of 2.15 seconds.

Figures (9-a) and (9-b) show the system response for the first strategy for K_p = 15 and K_p = 10 respectively, where the system in this range gives more satisfactory dynamic response. Increasing the gain from 10 to 15 reduces the error from about 19 r.p.m. to about 10 r.p.m. but with a corresponding increase in system oscillations. Figure (9-a) shows the case where duty cycle reaches its saturation value (λ = 1.0) and remains there for some before starting to reduce. Figure (9-b) shows the situation where duty cycle just reaches 1.0. Table (1) shows comparison of response specifications for the two cases for the first startegy.

where,

M_p : percentage maximum overshoot
e_{ss} : percentage steady-state error
t_r : Rise time
t_p : Peak time
t_d : Delay time

Figures (10a) and (10b) show the system response for the second strategy for K_p = 6 and K_p = 1.9 respectively. Figure (10a) shows the case where duty cycle reaches its saturation value (λ = 1.0) and remains there for some time depending on the system reaching its peak speed. Figure (10b) shows the case where duty cycle just reaches 1.0. Table (2) shows comparison of response specifications for the two cases for the second strategy.

Table 1. Comparison of Response specifications for first startegy.

K_p = 15					K_p = 10				
M_p	e_{ss}	t_r	t_p	t_d	M_p	e_{ss}	t_r	t_p	t_d
44%	1.08%	33.7 ms	101.7 ms	15.7ms	34%	2%	54.8 ms	119.7 ms	22.7 ms

Table 2. Comparison of Response specifications for second startegy.

K_p = 6					K_p = 1.9				
M_p	e_{ss}	t_r	t_p	t_d	M_p	e_{ss}	t_r	t_p	t_d
9.6%	1.56%	266 ms	335 ms	155.8 ms	0	3.77%	-------	--------	-------

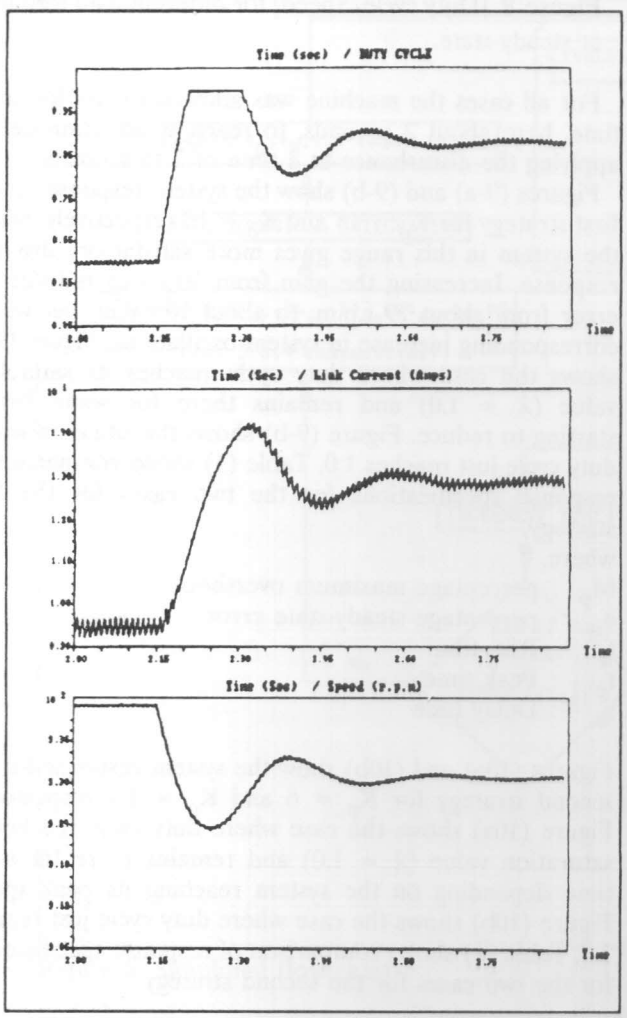

Figure 9a. Dynamic response for first strategy [K_p = 15].

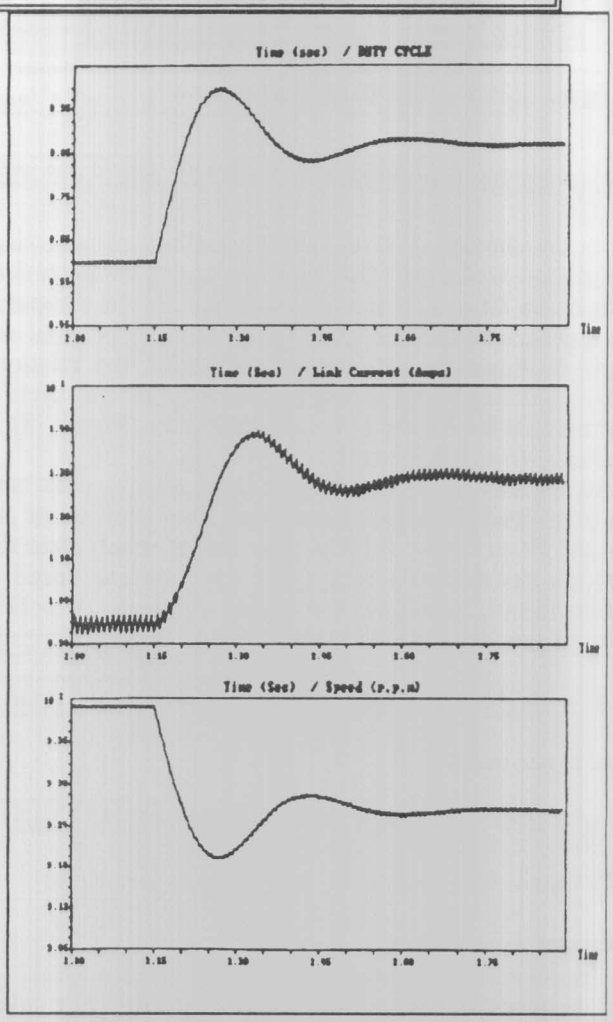

Figure 9b. Dynamic response for first strategy [K_p = 10]

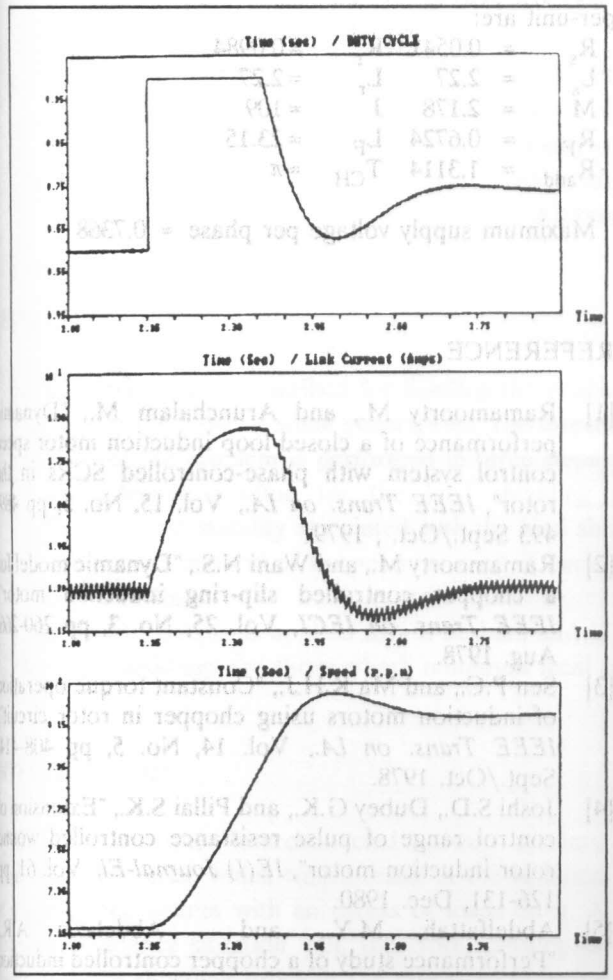

Figure 10a. Dynamic response for second strategy - [K_p = 6]

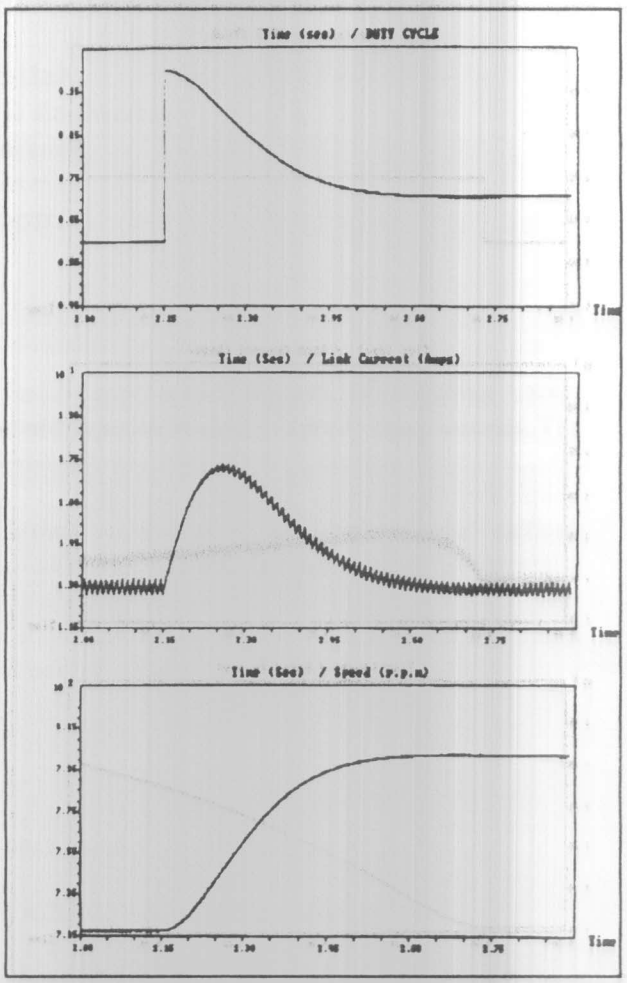

Figure 10b. Dynamic response for second strategy - [K_p = 1.9]

To emphasize the effect of feedback control on the system response, an open-loop operation was studied for the sake of comparison. Figure (11) shows the system response for the open-loop operation. These results were for the case where the system was working as a variable speed drive with load torque T_L = 8 N.m and chopper duty cycle changed manually from 0.6 to 0.75 at a time of 2.15 sec. to chieve a steady-state speed of 833 r.p.m. Figure (11) shows a very poor response for open-loop operation when compared with Figures (10a) and (10b) using the closed-loop controller.

CONCLUSIONS

The system studied previously in reference [5] was the scope of this paper by introducing a closed-loop controller. Analysis and simulation consider the induction motor equations from the rotor side where a diode bridge is connected and where one should find the convenience of solving these equations taking the noinlinear devices (diodes) into account. The analysis used gives us precise calculations for all system states without introducing any approximations.

The system response with a closed-loop controller following large signal perturbations was predicted. A proportional controller was used for this study. An improved system response was achieved. However, steady-state error was present. This steady-state error was due to the fact that the system is of type 0, one with no factors of s in the denominator of the transfer function. To eliminate this steady-state error an integral action can be added to the controller. Also, to increase the effective damping, a derivative action could be incorporated in conjunction with either a proportional or proportional plus integral controller.

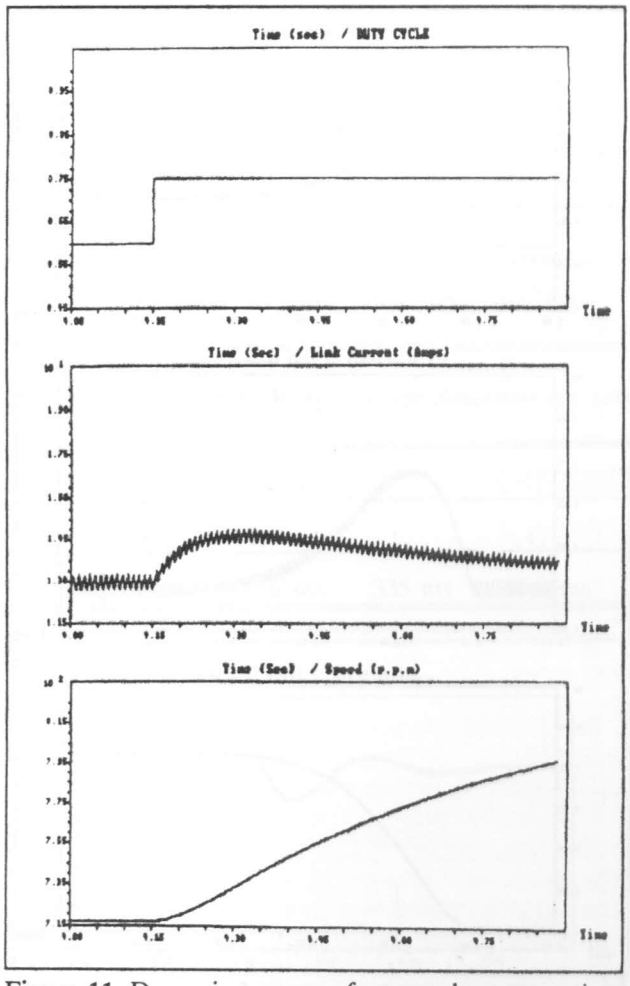

Figure 11. Dynamic response for open-loop operation.

APPENDIX (A)

The machine used has 4 poles. The base quantities used are as follows:

I_{base} = 31.94 Amps. (peak rated rotor current per phase)
V_{base} = 89.30 Volts (peak rated rotor voltage per phase)
f_{base} = 50 Hz
$\omega_{base} = 2\pi f_{base}$ = 314.16 elec. rad/sec
$T_{base} = 1/\omega_{base}$ = 0.003183 sec.
$Z_{base} = V_{base}/I_{base}$ = 2.796 Ohms
$L_{base} = Z_{base}/\omega_{base}$ = 8.9 mH
$Power_{base} = (3/2)\, V_{base}\, I_{base}$ = 4278.4 Watts
$\omega_{m\text{-}base} = \omega_{base}/2$ = 157.08 mech. rad/sec
$Torque_{base} = Power_{base}/\omega_{m\text{-}base}$ = 27.24 N.m
$J_{base} = Torque_{base} \times (T_{base}/\omega_{m\text{-}base})$
$= 5.52 \times 10^{-4}$ Kg.m^2

Using these basee quantities, the system parameters in per-unit are:

R_s	= 0.0541	R_r	= 0.0984
L_s	= 2.27	L_r	= 2.27
M	= 2.178	J	= 109
R_F	= 0.6724	L_F	= 23.15
R_{add}	= 1.3114	T_{CH}	= π

Maximum supply voltage per phase = 0.7368

REFERENCE

[1] Ramamoorty M., and Arunchalam M., "Dynamic performance of a closed loop induction motor speed control system with phase-controlled SCRs in the rotor", *IEEE Trans. on IA.*, Vol. 15, No. 5, pp 489-493 Sept./Oct. , 1979.

[2] Ramamoorty M., and Wani N.S., "Dynamic model for a chopper controlled slip-ring induction motor", *IEEE Trans. on IECI*, Vol. 25, No. 3, pp 260-266, Aug. 1978.

[3] Sen P.C., and Ma K.H.J., "Constant torque operation of induction motors using chopper in rotor circuit", *IEEE Trans. on IA.*, Vol. 14, No. 5, pp 408-414, Sept./Oct. 1978.

[4] Joshi S.D., Dubey G.K., and Pillai S.K., "Extension of control range of pulse resistance controlled wound rotor induction motor", *IE(I) Journal-EI*, Vol. 61, pp 126-131, Dec. 1980.

[5] Abdelfattah M.Y., and Abdelaziz A.R., "Performance study of a chopper controlled induction motor using tensor technique", *Alexandria Engineering Jornal*, Vol. 29, No. 2, Section B, pp. 33-41, April 1990.

[6] Hancock N.N., "*Matrix Analysis of Electrical Machinery*", Pergamon Press, Second Edition, Chapter 7, 1974.

[7] Stagg G.W., El-Abiad A.H., "*Computer Method in Power System Analysis*", McGraw-Hill Kogakusha, Chapter 8, 1968.

[8] Williams S., and Smith I.R., "Fast digital computation of 3-phase thyristor bridge circuits", *Proc. IEE*, Vol. 120 No. 7, pp 791-795, July 1973.

[9] Abdelfattah M.Y., "Converter simulation with special reference to power system disturbance", *Ph.D. Thesis*, UMIST, England, 1985.

[10] Kuo B.C., "*Automatic Control System* " Prentice-Hall of India, Fourth Edition, Chapter 6, pp 308-383, 1983.